Chapter 3

Newly Designed Slider Bearing with Inclined Pad Surface Including Effects of Porosity, Anisotropic Permeability, Slip Velocity at Both the Ends and Squeeze Velocity

Contents

3.1 Introduction

Wu [108] in an innovative analysis, dealt with the case of squeeze film behaviour for porous annular disks in which he showed that owing to the fact that fluid can flow through the porous material as well as through the space between the bounding surfaces, the performance of a porous walled squeeze film can differ substantially from that of a solid walled squeeze film. Later [96] extended the above analysis [108] by introducing the effect of velocity slip to porous walled squeeze film with porous matrix appeared in the above plate. They found that the load capacity decreases due to the effect of porosity and slip. Prakash and Vij [67] investigated a porous inclined slider bearing without the effect of magnetic fluid (MF) and found that porosity caused decrease in the load capacity and friction, while it increased the coefficient of friction. Gupta and Bhat [25] found that the load capacity and friction could be increased by using a transverse magnetic field on the bearing and a conducting lubricant.

With the advent of ferrofluid (FF), Agrawal [1] studied its effects on a porous inclined bearing and found that the magnetizing of particles in the lubricant increased its load capacity without affecting the friction on the moving slider. Recently, many authors [71, 76, 80, 81, 83, 85, 91, 95, 100] have analyzed effects of FF as lubricant in their study and found the increase of efficiency of the bearing performance over conventional from different viewpoints.

In all above investigations, none of the authors considered both the porous plates (or discs or surfaces) in their study. The porous layer (or matrix or region) in the bearing is considered because of its advantageous property of self lubrication. With this motivation the study of behaviour of an inclined slider bearing with the porous matrix attached to both the plates (that is upper and lower) is proposed here with a FF lubricant under a magnetic field oblique to the lower surface. Also, effects of slip velocity and anisotropic permeability at both the porous plates, as well as squeeze velocity when the upper plate approaches to lower one are included. The FF flow model considered here is due to R. E. Rosensweig [74].

A FF lubrication model is derived for the above problem and the various sizes of upper and lower porous matrix are considered for computation of various bearing characteristics like load capacity, friction, coefficient of friction and center of pressures. Also, above characteristics have

been computed for two different cases of anisotropic permeabilities at upper and lower porous matrix. The FF used in the computations is water based.

3.2 Formulation of the Mathematical Model

A schematic diagram of the system under study is presented in Figure 3.1 consists of a FF film of thickness h within an inclined pad surface (stator) and a slider of length A in the *x*- direction and width B in *y*- direction, $A \ll B$. The value of h is h_2 at the inlet and h_1 at the outlet. This film thickness is given by

$$h = h_2 - \frac{(h_2 - h_1)x}{A}.$$

… (3.1)

The slider and stator both have attached porous matrix of thickness l_2 and l_1 respectively. Both the porous matrix are backed by a solid wall. The slider moves with a uniform velocity U in the *x*- direction. Also, stator moves normally towards the slider with a uniform velocity $\dot{h} = dh/dt$, where *t* is time.

By combining equations (2.11) to (2.15) under the usual assumption of lubrication, neglecting inertia terms and that the derivatives of velocities across the film predominate, the equation governing the lubricant flow in the film region yields

$$\frac{\partial^2 u}{\partial z^2} = \frac{1}{\eta}\frac{\partial}{\partial x}\left(p - \frac{1}{2}\mu_0\,\bar{\mu}\,H^2\right),$$

… (3.2)

where u is the film fluid velocity in the *x*- direction and H is the magnetic field strength, p is fluid pressure in fluid film region, μ_0 is free space permeability, $\bar{\mu}$ is magnetic susceptibility, η is fluid viscosity and x, z are axial coordinates.

Solving equation (3.2) under the slip boundary conditions given by Sparrow *et.al*. [96] and modified by Shah *et.al*. [80] with the addition of slider velocity U to [96]

$$u = \frac{1}{s_1}\frac{\partial u}{\partial z} + U \text{ when } z = 0 \text{ and } \quad u = -\frac{1}{s_2}\frac{\partial u}{\partial z} \text{ when } z = h,$$

… (3.3)

where

$$\frac{1}{s_1} = \frac{\sqrt{\varphi_x \eta_x}}{5} \text{ and } \frac{1}{s_2} = \frac{\sqrt{\psi_x m_x}}{5} \ ;$$

… (3.4)

$\frac{1}{s_1}$, $\frac{1}{s_2}$ being slip parameters, η_x, m_x are porosities in the *x*- direction and φ_x, ψ_x are permeabilities in the *x*- direction in the porous region.

The equation (3.2) becomes

$$u = \frac{1}{\eta}\left[\frac{z^2}{2} - \frac{h s_1 s_2 z}{s}\left(\frac{h}{2} + \frac{1}{s_2}\right) - \frac{h s_2}{s}\left(\frac{h}{2} + \frac{1}{s_2}\right)\right]\frac{\partial}{\partial x}\left(p - \frac{1}{2}\mu_0\,\bar{\mu}\,H^2\right) + \frac{s_1 s_2}{s}\left[\left(\frac{1}{s_2} + h\right) - z\right]U,$$

… (3.5)

where

$$s = s_1 + s_2 + h s_1 s_2.$$

… (3.6)

Substituting the above value of u in the integral form of continuity equation

$$\frac{\partial}{\partial x}\int_0^h u\, dz + w_h - w_0 = 0,$$

… (3.7)

where w is the axial component of the fluid velocity in the film, w_h and w_0 are values of w at $z = h$ and $z = 0$ respectively.

One obtains

$$\frac{\partial}{\partial x}\left[\frac{1}{\eta}\left\{\frac{h^3}{6}-\frac{s_1 s_2 h^3}{2s}\left(\frac{h}{2}+\frac{1}{s_2}\right)-\frac{s_2 h^2}{s}\left(\frac{h}{2}+\frac{1}{s_2}\right)\right\}\frac{\partial}{\partial x}\left(p-\frac{1}{2}\mu_0\,\bar{\mu}\,H^2\right)+\frac{h s_1 s_2 U}{s}\left(\frac{1}{s_2}+\frac{h}{2}\right)\right]$$

$$+w_h - w_0 = 0.$$

… (3.8)

Using Darcy's law, the velocity components of the fluid in the porous matrix are given as follow:

For upper porous region:

$$\bar{u}_1 = -\frac{\psi_x}{\eta}\frac{\partial}{\partial x}\left(P-\frac{1}{2}\mu_0\,\bar{\mu}\,H^2\right), \text{(in } x\text{- direction)}$$

… (3.9)

$$\bar{w}_1 = -\frac{\psi_z}{\eta}\frac{\partial}{\partial z}\left(P-\frac{1}{2}\mu_0\,\bar{\mu}\,H^2\right), \text{(in } z\text{- direction)}$$

… (3.10)

where ψ_x, ψ_z are fluid permeabilities in the upper porous region in x and z- direction respectively, and P is the fluid pressure in the porous region.

For lower porous region:

$$\bar{u}_2 = -\frac{\varphi_x}{\eta}\frac{\partial}{\partial x}\left(P-\frac{1}{2}\mu_0\,\bar{\mu}\,H^2\right), \text{(in } x\text{- direction)}$$

… (3.11)

$$\bar{w}_2 = -\frac{\varphi_z}{\eta}\frac{\partial}{\partial z}\left(P-\frac{1}{2}\mu_0\,\bar{\mu}\,H^2\right), \text{(in } z\text{- direction)}$$

… (3.12)

where φ_x, φ_z are fluid permeabilities in the lower porous region in x and z- direction respectively, and P is the fluid pressure in the porous region.

Substituting equations (3.9) and (3.10) in the continuity equation for upper porous region

$$\frac{\partial \bar{u}_1}{\partial x} + \frac{\partial \bar{w}_1}{\partial z} = 0,$$

… (3.13)

yields

$$\frac{\psi_x}{\eta}\frac{\partial^2}{\partial x^2}\left(P - \frac{1}{2}\mu_0\,\bar{\mu}\,H^2\right) + \frac{\psi_z}{\eta}\frac{\partial^2}{\partial z^2}\left(P - \frac{1}{2}\mu_0\,\bar{\mu}\,H^2\right) = 0,$$

… (3.14)

which on integration with respect to z across the upper porous matrix $(h, h + l_1)$, one obtains

$$\frac{\psi_z}{\eta}\frac{\partial}{\partial z}\left(P - \frac{1}{2}\mu_0\,\bar{\mu}\,H^2\right)\Big|_{z=h} = \frac{\psi_x}{\eta}\frac{\partial^2}{\partial x^2}\left(p - \frac{1}{2}\mu_0\,\bar{\mu}\,H^2\right) l_1,$$

… (3.15)

using Morgan-Cameron approximation [67, 81] and that the surface $z = h + l_1$ is non-porous.

Substituting equations (3.11) and (3.12) in the continuity equation for lower porous region

$$\frac{\partial \bar{u}_2}{\partial x} + \frac{\partial \bar{w}_2}{\partial z} = 0,$$

… (3.16)

yields

$$\frac{\varphi_x}{\eta}\frac{\partial^2}{\partial x^2}\left(P - \frac{1}{2}\mu_0\,\bar{\mu}\,H^2\right) + \frac{\varphi_z}{\eta}\frac{\partial^2}{\partial z^2}\left(P - \frac{1}{2}\mu_0\,\bar{\mu}\,H^2\right) = 0,$$

… (3.17)

which on integration with respect to z across the upper porous matrix $(-l_2, 0)$, one obtains

$$\frac{\varphi_z}{\eta}\frac{\partial}{\partial z}\left(P - \frac{1}{2}\mu_0\,\bar{\mu}\,H^2\right)\Big|_{z=0} = -\frac{\varphi_x}{\eta}\frac{\partial^2}{\partial x^2}\left(p - \frac{1}{2}\mu_0\,\bar{\mu}\,H^2\right) l_2,$$

… (3.18)

using Morgan-Cameron approximation [67, 81] and that the surface $z = -l_2$ is non-porous.

Considering the normal component of velocity across the film porous interface are continuous, so that $w_h = \dot{h} + \overline{w}_1$, $w_0 = \overline{w}_2$, equations (3.15), (3.18) and (3.8) yields

$$\frac{\partial}{\partial x}\left[g^* \frac{\partial}{\partial x}\left(p - \frac{1}{2}\mu_0\, \bar{\mu}\, H^2\right)\right] = \frac{\partial e^*}{\partial x},$$

… (3.19)

where

$$g^* = \frac{1}{12s\eta}\left[h^2(12 + 4hs_1 + 4hs_2 + h^2 s_1 s_2) + 12s(\psi_x l_1 + \varphi_x l_2\right],$$

$$e^* = \frac{Uhs_1}{2s}(2 + hs_2) + x\dot{h},$$

which is the Reynolds's type equation for the considered phenomenon.

By considering magnetic field strength which vanish at the inlet and outlet as

$$H^2 = Kx(A - x),$$

… (3.20)

where K being a quantity chosen to suit the dimensions of both sides of equation (3.20).

Such a magnetic field attains a maximum at the middle of the bearing producing magnetic pressure. On the other hand a uniform magnetic field cannot produce magnetic pressure because $dH^2/dx = 0$.

Introducing the dimensionless quantities

$$X = \frac{x}{A}, \quad \bar{h} = \frac{h}{h_1}, \quad \overline{\psi}_x = \frac{\psi_x}{h_1^2}, \quad \overline{\psi}_z = \frac{\psi_z}{h_1^2}, \quad \bar{\varphi}_x = \frac{\varphi_x}{h_1^2}, \quad \bar{\varphi}_z = \frac{\varphi_z}{h_1^2},$$

$$\bar{l}_1 = \frac{l_1}{h_1}, \quad \bar{l}_2 = \frac{l_2}{h_1}, \quad \bar{s}_1 = s_1 h_1, \quad \bar{s}_2 = s_2 h_1, \quad \bar{p} = \frac{p h_1^2}{AU\eta},$$

$$\mu^* = \frac{\mu_0\, \bar{\mu}\, KAh_1^2}{U\eta}, \quad S = -\frac{2A\dot{h}}{Uh_1},$$

equations (3.1) and (3.20) implies respectively

$$\bar{h} = \frac{h_2 - (h_2 - h_1)X}{h_1}; \;\; 0 \le X \le 1,$$

and

$$H^2 = KA^2X(1 - X).$$

Also, equation (3.19) transforms to

$$\frac{d}{dX}\left[G^* \frac{d}{dX}\left(\bar{p} - \frac{1}{2}\mu^* X(1 - X)\right)\right] = \frac{dE^*}{dX},$$

… (3.21)

where

$$G^* = \bar{h}^2\left(12 + 4\bar{h}\,\bar{s}_1 + 4\bar{h}\,\bar{s}_2 + \bar{h}^2\bar{s}_1\bar{s}_2\right) + 12\,\bar{s}\left(\bar{\psi}_x\bar{l}_1 + \bar{\varphi}_x\bar{l}_2\right),$$

$$E^* = -6\,\bar{s}\,S\,X + 6\,\bar{s}_1\bar{h}\left(2 + \bar{s}_2\bar{h}\right).$$

Equation (3.21) is known as dimensionless Reynolds's type equation.

3.3 Expressions of Bearing Characteristics

Since the pressure is negligible on the boundaries of the slider bearing compared to inside pressure, solving equation (3.21) under boundary conditions $\bar{p} = 0$ when $X = 0,\ 1$.

The dimensionless film pressure $\bar{p}$ is obtained as:

$$\bar{p} = \frac{1}{2}\mu^* X(1 - X) + \int_0^X \left(\frac{E^* - Q}{G^*}\right) dX,$$

where

$$Q = \int_0^1 \left(\frac{E^*}{G^*}\right) dX \Big/ \int_0^1 \left(\frac{1}{G^*}\right) dX.$$

The load carrying capacity W, friction on the moving slider F, coefficient of friction f and the *x*- coordinate of the center of pressure Y are expressed respectively in dimensionless forms as

$$\overline{W} = \frac{W h_1^2}{BU\eta A^2} = \frac{\mu^*}{12} - \int_0^1 \left(\frac{E^* - Q}{G^*}\right) X \, dX,$$

$$\bar{F} = -\frac{F h_1}{BUA\eta} = \int_0^1 \frac{\bar{h}\,\bar{s}_1(2 + \bar{h}\,\bar{s}_2)}{2\bar{s}} \left(\frac{E^* - Q}{G^*}\right) dX + \int_0^1 \frac{\bar{s}_1\,\bar{s}_2}{\bar{s}}\, dX,$$

$$\bar{f} = \frac{Af}{h_1} = \frac{\bar{F}}{\overline{W}},$$

$$Y = \frac{\bar{X}}{A} = \frac{1}{\overline{W}} \left[\frac{\mu^*}{24} - \frac{1}{2}\int_0^1 \left(\frac{E^* - Q}{G^*}\right) X^2 \, dX\right],$$

where

$$W = \int_0^B \int_0^A p \, dxdy$$

and

$$F = \eta \int_0^B \int_0^A \left(\frac{\partial u}{\partial z}\right)_{z=0} dxdy.$$

3.4 Calculation of Results

The various bearing characteristics like load capacity, frictional force on the moving slider, the coefficient of friction and *x*- coordinate of center of pressure are computed for various sizes of upper and lower porous matrix for $\varphi_x = 0.00001$, $\psi_x = 0.001$ and for $\varphi_x = 0.001$, $\psi_x = 0.00001$, using Simpson's one-third rule with step size 0.1, for the following values of the parameters:

$$K = 10^9(A^2/m^4),\ \ A = 0.15(m),\ \ \eta = 0.012(Ns/m^2),$$
$$\eta_x = 0.64,\ \ m_x = 0.81,\ \ \mu_0 = 4\pi \times 10^{-7}(N/A^2),\ \ \bar{\mu} = 0.05,$$
$$U = 1.0(m/s),\ \ \dot{h} = -0.005(m/s),\ \ h_1 = 0.05(m),\ \ h_2 = 0.1(m).$$

3.5 Discussion of Results

The mathematical model of water based FF lubricated slider bearing with an inclined pad surface including combined effects of porosity, anisotropic permeability, slip velocity at both the ends, and squeeze velocity is proposed under an oblique magnetic field. The results of various bearing characteristics (refer Section 3.3) are obtained for the various values of the parameters (refer Section 3.4) are presented graphically.

From the Figures 3.2-3.9 the following observations are made:

In Figures 3.2 and 3.3, the dimensionless load capacity $\overline{W}$ for various values of lower porous matrix $\bar{l}_2$ and values of upper porous matrix $\bar{l}_1$ are displayed for the constant values of $\varphi_x = 0.00001$, $\psi_x = 0.001$ and $\varphi_x = 0.001$, $\psi_x = 0.00001$, respectively.

It is observed from the Figure 3.2 that the dimensionless load capacity decreases with the increase of porous matrix thickness $\bar{l}_2$ as well as $\bar{l}_1$. The decrease rate of load capacity is slow with respect to $\bar{l}_2$. It is observed from Figure 3.3 that, the dimensionless load capacity decreases with respect to $\bar{l}_2$ but its behaviour is almost remains same with respect to $\bar{l}_1$. The maximum dimensionless load capacity is obtained when $\bar{l}_1 = \bar{l}_2 = 0$ but with the disadvantage that the bearing has no self lubricating property. This behaviour of decrease in load capacity with the insertion of porous matrix also agrees with the conclusions of [67, 96]. According to [96] the above trends for squeeze film bearing can be obtained because of the physical process as under:

The presence of the porous medium provides a path for the fluid to come out easily form the slider bearing to the environment. The higher the permeability, the more readily does fluid flow through the porous material. Thus, the presence of the porous material decreases the resistance to flow in *x*- direction and as a consequence the load carrying capacity is reduced. The effect of

velocity slip is to decrease the resistance encountered by the fluid flowing in the gap itself and, by this means, to diminish the load carrying capacity.

In Figures 3.4 and 3.5, the dimensionless friction force on the moving slider $\bar{F}$ for various values of lower porous matrix $\bar{l}_2$ and values of upper porous matrix $\bar{l}_1$ are displayed for the constant values of $\varphi_x = 0.00001$, $\psi_x = 0.001$ and $\varphi_x = 0.001$, $\psi_x = 0.00001$, respectively.

It is observed that the same behaviour is obtained for $\bar{F}$ as we have discussed for $\bar{W}$ with respect to $\bar{l}_1$ and $\bar{l}_2$.

In Figures 3.6 and 3.7, the dimensionless coefficient of friction $\bar{f}$ for various values of lower porous matrix $\bar{l}_2$ and the values of upper matrix $\bar{l}_1$ are displayed for the constant values of $\varphi_x = 0.00001$, $\psi_x = 0.001$ and $\varphi_x = 0.001$, $\psi_x = 0.00001$, respectively.

It is observed that $\bar{f}$ increase with the increase of $\bar{l}_1$ and $\bar{l}_2$.

In Figures 3.8 and 3.9, the dimensionless x- coordinate of the center of pressure Y for various values of lower porous matrix $\bar{l}_2$ and the values of upper porous matrix $\bar{l}_1$ are displayed for the constant values of $\varphi_x = 0.00001$, $\psi_x = 0.001$ and $\varphi_x = 0.001$, $\psi_x = 0.00001$, respectively.

It is observed that the position of the center of pressure does not affect much with respect to $\bar{l}_1$ and $\bar{l}_2$.

Also, one can obtain the following cases for the specific values of the parameters:

(a) When $l_1 = 0$, $\dot{h} = 0$, the case of [85] is obtained from equation (3.21) as

$$\frac{d}{dX}\left[G^* \frac{d}{dX}\left(\bar{p} - \frac{1}{2}\mu^* X(1-X)\right)\right] = \frac{dE^*}{dX},$$

where

$$G^* = \bar{h}^2\left(12 + 4\bar{h}\,\bar{s}_1 + 4\bar{h}\,\bar{s}_2 + \bar{h}^2\bar{s}_1\bar{s}_2\right) + 12\,\bar{s}\,\bar{\varphi}_x\bar{l}_2\,,$$

$$E^* = 6\,\bar{s}_1\bar{h}\,(2 + \bar{s}_2\bar{h}).$$

(b) When $\mu^* = 0$, the non-ferrofluid case [67] is obtained from equation (3.21) as

$$\frac{d}{dX}\left[G^*\left(\frac{d\bar{p}}{dX}\right)\right] = \frac{dE^*}{dX},$$

where

$$G^* = \bar{h}^2\left(12 + 4\bar{h}\,\bar{s}_1 + 4\bar{h}\,\bar{s}_2 + \bar{h}^2\bar{s}_1\bar{s}_2\right) + 12\,\bar{s}\,(\bar{\psi}_x\bar{l}_1 + \bar{\varphi}_x\bar{l}_2),$$

$$E^* = -6\,\bar{s}\,S\,X + 6\,\bar{s}_1\bar{h}\,(2 + \bar{s}_2\bar{h}).$$

3.6 Conclusion

The present study proposes the mathematical model of water based FF lubricated slider bearing with an inclined pad surface including combined effects of porosity, anisotropic permeability, slip velocity at both the ends, and squeeze velocity under an oblique magnetic field. The results of various bearing characteristics are presented graphically.

The porous layer in the bearing is considered because of its advantageous property of self lubrication. With this motivation the present study is proposed.

Based upon the formulation in Section 3.2, and Results & discussion (Section 3.4 and 3.5) the following conclusions can be made for designing slider bearing:

(1) Because of having the self lubrication property of the porous plate bearings, it is suggested to have both the porous plate for better self lubrication.
(2) Better load capacity is obtained when the thickness of l_1 and l_2 are small.
(3) Small thickness of l_2 has more influence on better load capacity when $l_1 = 0$ and $\varphi_x = 0.00001$, $\psi_x = 0.001$.
(4) Small thickness of l_1 has more influence on better load capacity when $l_2 = 0$ and $\varphi_x = 0.001$, $\psi_x = 0.00001$.
(5) It should be noted that a uniform magnetic field does not enhance the bearing characteristics in this model due to Rosensweig since $\partial H/\partial x = 0$ in equation (3.2).

3.7 Figures

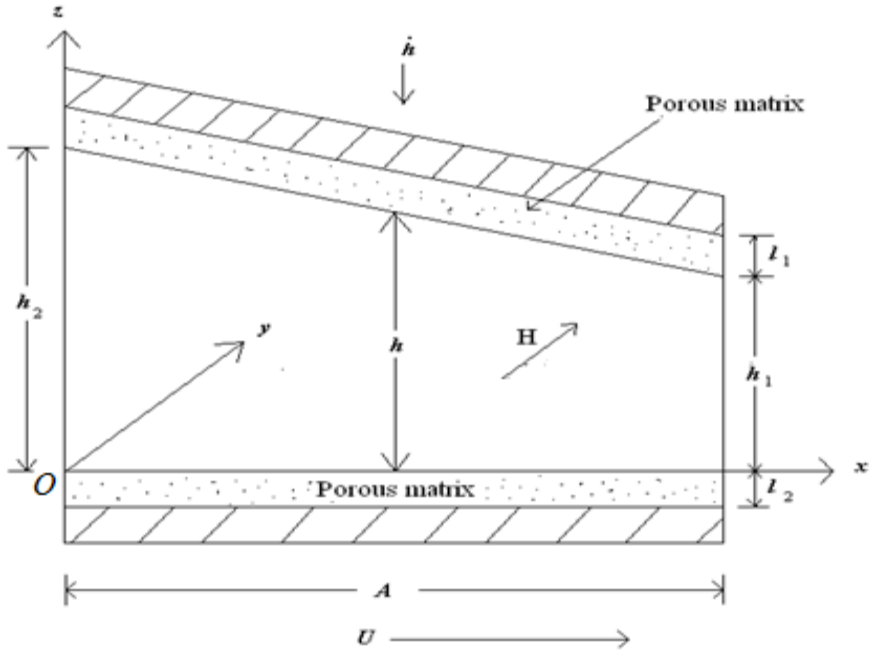

Figure 3.1 Slider bearing with inclined pad surface

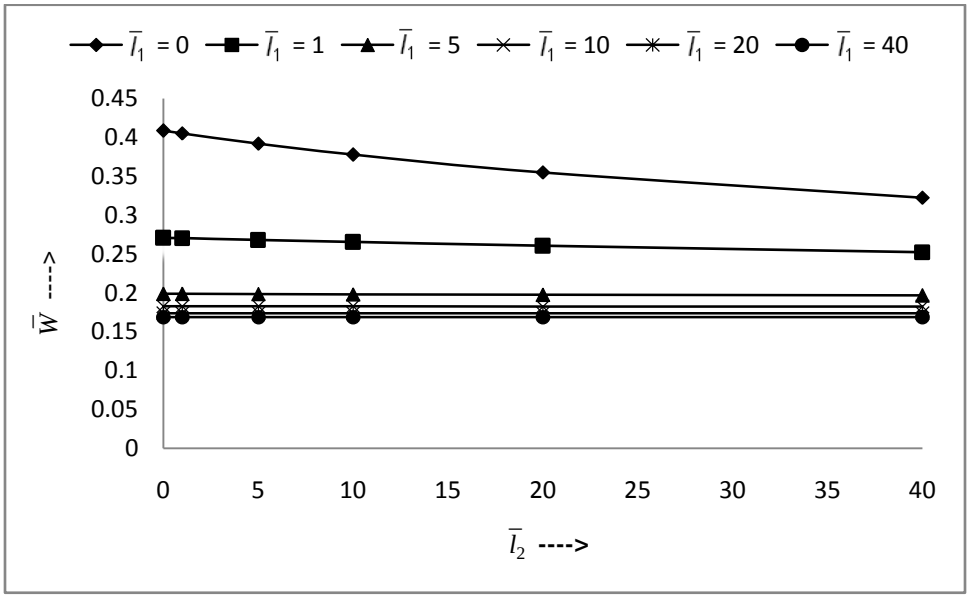

Figure 3.2 Dimensionless load capacity $\bar{W}$ for various values of $\bar{l}_1$ and $\bar{l}_2$ for $\varphi_x = 0.00001,\ \psi_x = 0.001$

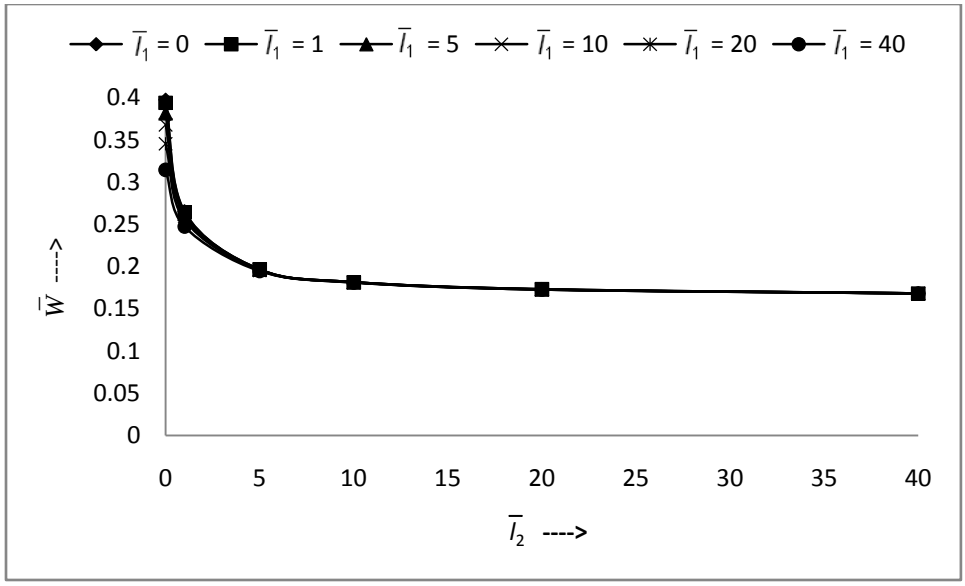

Figure 3.3 Dimensionless load capacity $\bar{W}$ for various values of $\bar{l}_1$ and $\bar{l}_2$ for $\varphi_x = 0.001$, $\psi_x = 0.00001$

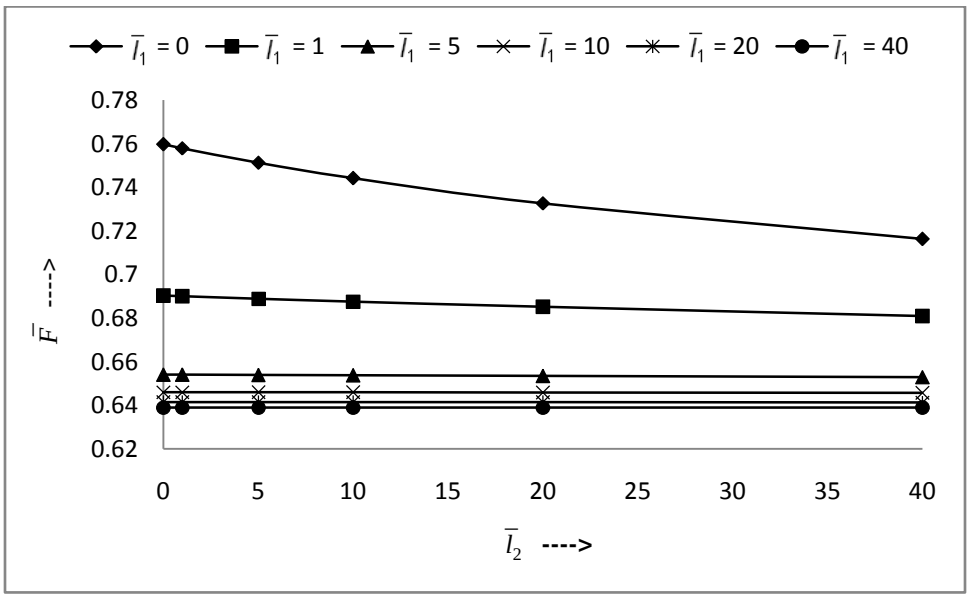

Figure 3.4 Dimensionless friction force on the moving slider $\bar{F}$ for various values of $\bar{l}_1$ and $\bar{l}_2$ for $\varphi_x = 0.00001$, $\psi_x = 0.001$

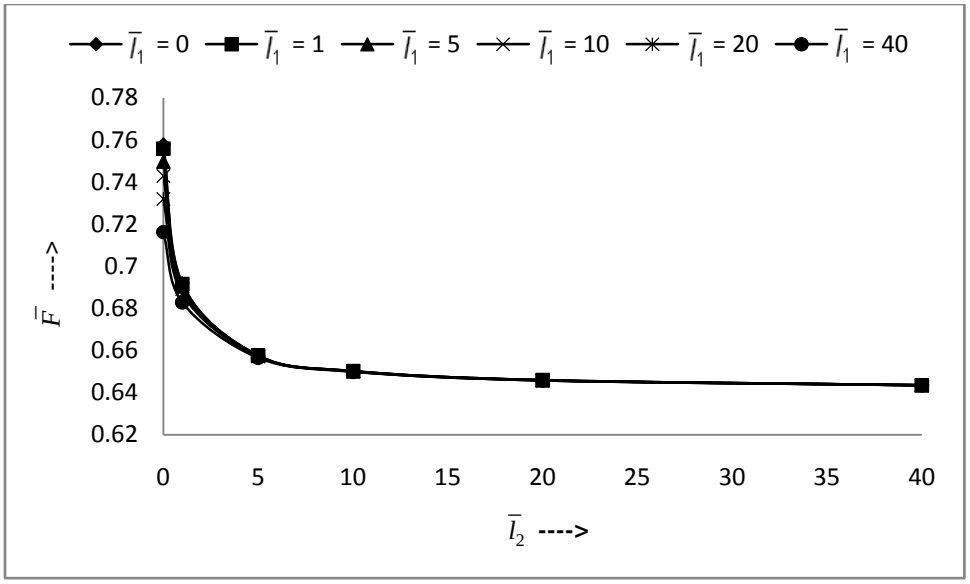

Figure 3.5 Dimensionless friction force on the moving slider $\bar{F}$ for various values of $\bar{l}_1$ and $\bar{l}_2$ for $\varphi_x = 0.001$, $\psi_x = 0.00001$

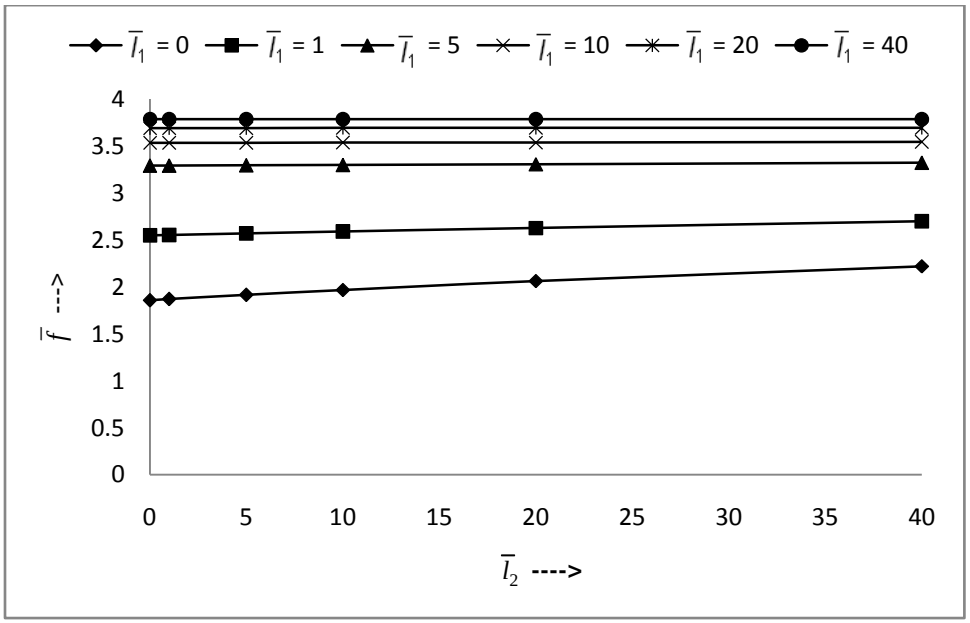

Figure 3.6 Dimensionless coefficient of friction $\bar{f}$ for various values of $\bar{l}_1$ and $\bar{l}_2$ for $\varphi_x = 0.00001$, $\psi_x = 0.001$

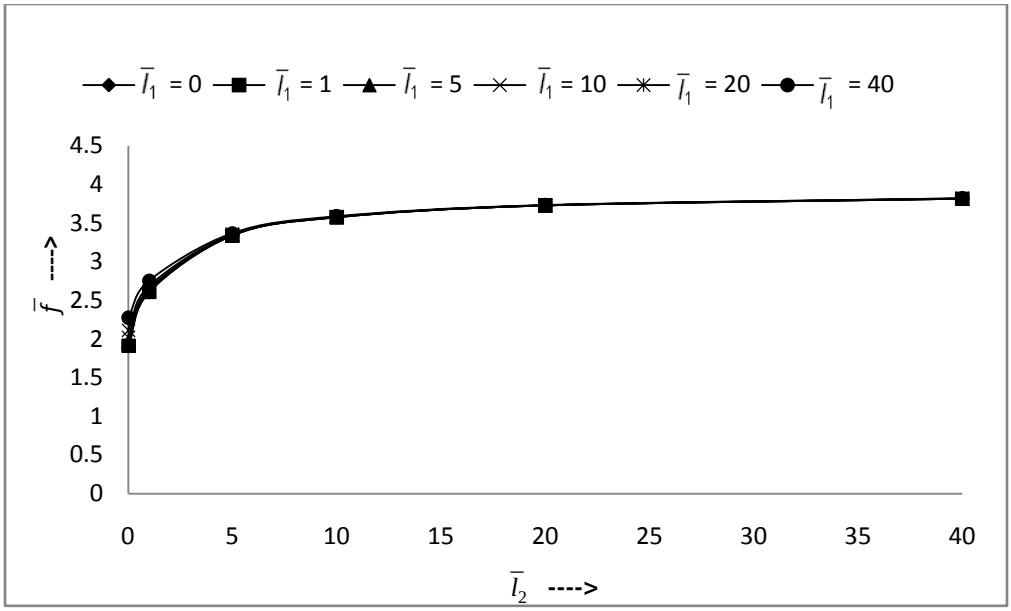

Figure 3.7 Dimensionless coefficient of friction $\bar{f}$ for various values of $\bar{l}_1$ and $\bar{l}_2$ for $\varphi_x = 0.001$, $\psi_x = 0.00001$

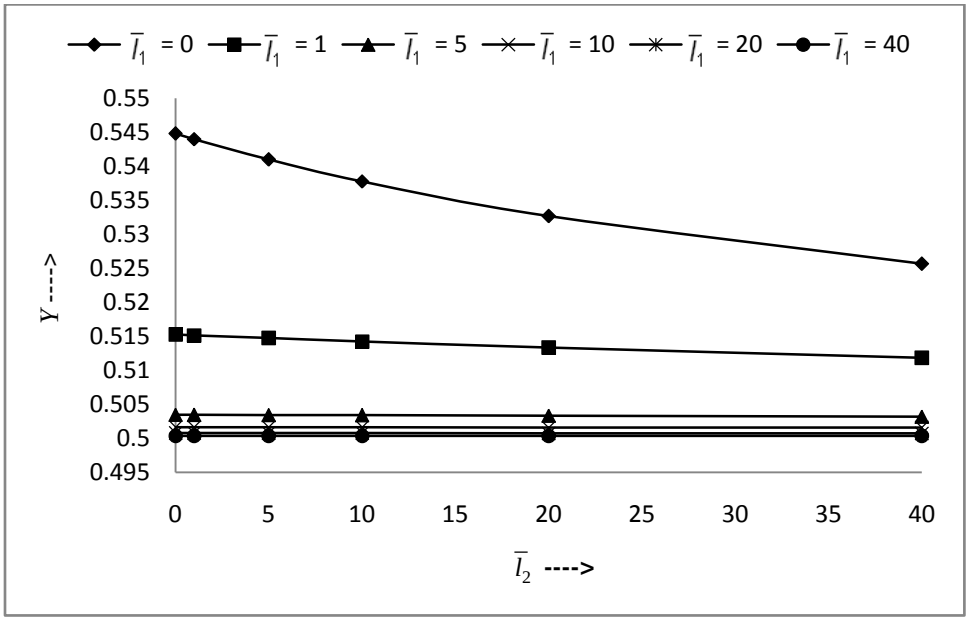

Figure 3.8 Dimensionless the x- coordinate of the center of pressure Y for various values of $\bar{l}_1$ and $\bar{l}_2$ for $\varphi_x = 0.00001$, $\psi_x = 0.001$

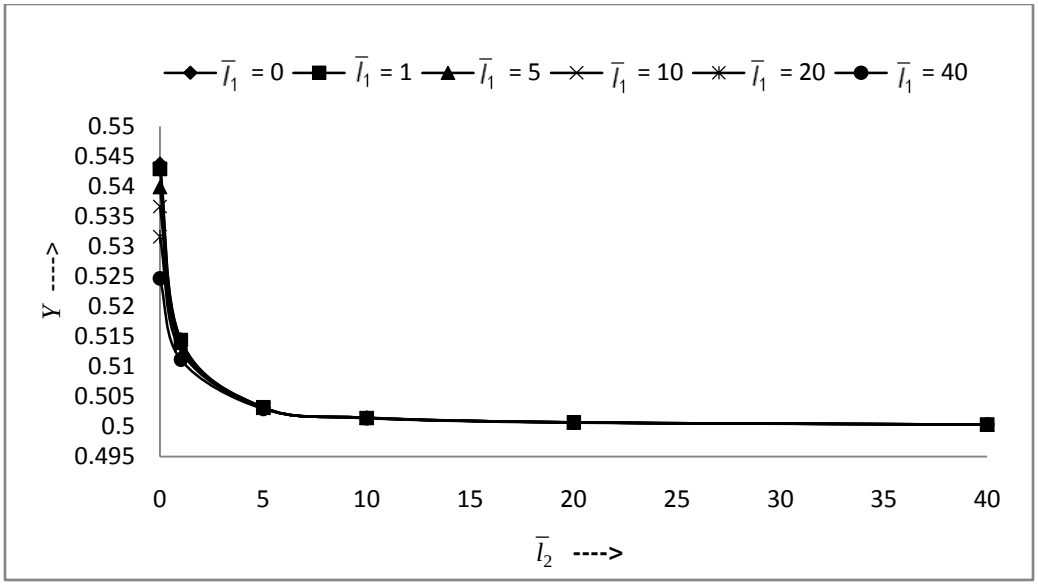

Figure 3.9 Dimensionless the x- coordinate of the center of pressure Y for various values of $\bar{l}_1$ and $\bar{l}_2$ for $\varphi_x = 0.001$, $\psi_x = 0.00001$